Hyperfine Interact
DOI 10.1007/s10751-011-0463-9

Evidence for a weakening 'dead zone' in Tokyo Bay over the past 30 years

Katsumi Shozugawa · Naoki Hara · Yutaka Kanai · Motoyuki Matsuo

Abstract Weakened hypoxia in the past 30 years at a dredged area in Tokyo Bay was proven by the existence of amorphous hematite (α-Fe2O3) in sediments. The chemical states of iron in sediments can become a proxy for the scale of anoxia at the time of sedimentation. In 2009, we collected core sediments from a dredged area off Makuhari in Tokyo Bay that is very strongly anoxic in the summer. Every layer of the sediments was analysed by ^{57}Fe Mössbauer spectroscopy and excess 210Pb dating, and amorphous hematite was identified in the sediments from the 1976–1979, 1986–1989 and 2006–2009 layers. Using an estimate based on the Eh-pH diagram optimized for the sedimental environment, the existence of hematite in the dredged area proves that the scale of hypoxia/anoxia is decreasing, and these results agree well with the observed dissolved oxygen level of the seawater mass.

Keywords ^{57}Fe Mössbauer spectroscopy · Sediments · Hypoxia · Hematite

1 Introduction

'Seas of death' (dead zones) with little dissolved oxygen (DO) in the bottom water mass have expanded since the 1960s on sea coasts all over the world and have greatly influenced ecosystems and inshore fisheries [1]. This study suggests that the chemical

K. Shozugawa (✉) · N. Hara · M. Matsuo
Graduate School of Arts and Sciences, The University of Tokyo,
3–8–1 Komaba, Meguro, Tokyo 153–8902, Japan
e-mail: cshozu@mail.ecc.u-tokyo.ac.jp

Y. Kanai
National Institute of Advanced Industrial Science and Technology,
1–1–1 Higashi, Tsukuba, Ibaraki 305–8567, Japan

Published online: 29 November 2011

states of iron in sediments are a proxy for redox conditions, including hypoxia. Because iron is one of the most abundant elements included in sediments, its various chemical states on an Eh-pH diagram have been clarified [2], and iron is expected to have taken the chemical state corresponding to the redox status of seawater.

Moreover, to estimate the scale of past hypoxia/anoxia, it is necessary to study areas where more strongly anoxic water has occurred in the summers. At the seabed in Tokyo Bay, vast dredged trenches have been formed sporadically along the coasts by reclamation of the foreshore since the 1970s [3]. Although the water depth of the coastal Tokyo Bay is between 5 and 10 metres, the water depth of some dredged trenches reaches 30 metres. In particular, the dredged trench off Makuhari has the maximum area and depth, and strong hypoxia has been observed there due to the stagnation of water currents [3]. Therefore, this area is suitable for an estimation of past hypoxia/anoxia. In this study, sediment cores were collected from the Makuhari dredged trench, and the relationship between chemical states of iron according to sedimentation age and DO at sedimentation were analysed by using ^{57}Fe Mössbauer spectroscopy and excess ^{210}Pb dating.

2 Experimental

The Mössbauer spectra were measured with an Austin Science S-600 spectrometer using a 1.11 GBq ^{57}Co/Rh source at room temperature. The Doppler velocity was set to ± 10.0 mm·sec^{-1} maximum. Gamma rays at 14.4 keV were collected from each sample for two or three days. Curves were fitted to the resulting spectra using a personal computer, assuming that the spectra were composed of peaks with Lorentzian line shapes. The half-widths and peak areas of each quadrupole doublet were constrained to be equal. Isomer shifts were expressed with respect to the centroid of the spectrum of metallic iron foil. The excess ^{210}Pb method was used for the age determination of the sediments [4].

3 Results and discussion

In the dredged trench, the seabed is muddy and some methane exhaust (φ *ca.* 10 cm) appears on the surface (point A, depth: 26 m). In contrast, the non-dredged seabed (point B, depth: 8 m) is sandy, and no methane exhaust is visible. Both cores were cut in the vertical direction every 3 cm immediately after sampling. In order to prevent oxidation by the air, all samples were put into clean and impenetrable bags, and various measurements such as ^{57}Fe Mössbauer measurements were started from the day of sampling.

Figure 1 shows the DO in the bottom water at point A and at an observatory (non-dredged) near the Tokyo light beacon. Seawater above the dredged trench had the following features: 1) vertical circulation tended to be weak in summer, and 2) horizontal currents are the same as in other areas. That is, the Makuhari dredged trench underwent a localized event suggesting rapid DO consumption such as that by microbial respiration.

^{57}Fe Mössbauer spectra at 0–3 cm and 3–6 cm in depth at point A are shown in Fig. 2, and the parameters for all sediment layers are given in Table 1. The spectrum

Fig. 1 Variation in DO over decades in the dredged area and at the Tokyo beacon

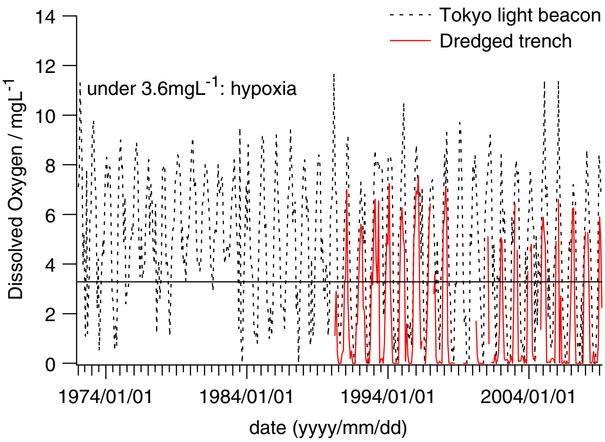

Fig. 2 ^{57}Fe Mössbauer spectra of sediments from dredged trench: spectra of the 0–3 cm layer (*top*) and the 3–6 cm layer (*bottom*)

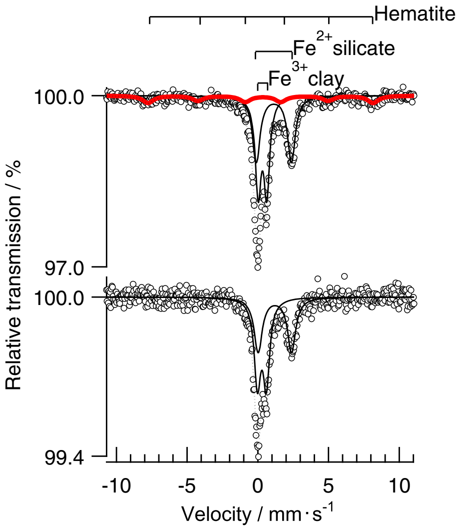

of surface sediment (0–3 cm) in Fig. 2 includes three species. Two kinds of doublet peaks at the centre of the spectrum are Fe^{3+}h.s. (δ 0.3 mm·s^{-1}, Δ 0.6 mm·s^{-1}) and Fe^{2+}h.s. (δ 1.1 mm·s^{-1}, Δ 2.4 mm·s^{-1}), which can be tentatively identified as clay minerals and silicate minerals, respectively. A value likely to be associated with hematite, which shows a sextet component, also appears. Hematite has distinctive features such as a δ value of +0.3 mm·s^{-1}, Δ of −0.2 mm·s^{-1} and hyperfine field H of 50 T. Hematite was observed only at point A at depths of 0–3 cm, 24–27 cm and 36–39 cm. However, at point B, hematite was observed in the samples at all layers. Hematite was not detected by x-ray diffraction (XRD, D8 Advance, Bruker) measurement in any layers, suggesting the presence of amorphous hematite in the sediments.

Hematite, which has a sextet component, is also the major chemical species, the generation conditions of which must be considered. The Eh-pH diagram for hematite

Table 1 ^{57}Fe Mössbauer parameters of all sediment layers

Sampling site	Layers / cm	Sedimentation age	Species	Area / %	I.S.(δ)/mm·s^{-1}	Q.S.(Δ)/mm·s^{-1}	H.W./mm·s^{-1}	H.I. / T
Dredged trench (Point A)	0–3	2007.7	Clay (Fe^{3+} h.s.)	43.24	0.328(5)	0.604(9)	0.496(12)	
			Silicate (Fe^{2+} h.s.)	40.53	1.135(8)	2.487(15)	0.656(24)	
			Hematite	16.23	0.279(40)	−0.176(78)	0.940(160)	49.27(30)
	3–6	2005.2	Clay (Fe^{3+} h.s.)	54.96	0.287(17)	0.632(35)	0.561(24)	
			Silicate (Fe^{2+} h.s.)	45.04	1.207(28)	2.365(57)	0.696(42)	
	6–9	2002.7	Fe3+ h.s.	100	0.284(28)	0.675(46)	0.502(72)	
	9–12	2000.2	Clay (Fe^{3+} h.s.)	72.67	0.296(26)	0.583(51)	0.695(54)	
			Silicate (Fe^{2+} h.s.)	27.33	1.204(33)	2.457(67)	0.445(65)	
	12–15	1997.7	Clay (Fe^{3+} h.s.)	53.75	0.322(25)	0.548(40)	0.555(61)	
			Silicate (Fe^{2+} h.s.)	46.25	1.148(35)	2.461(68)	0.663(79)	
	15–18	1995.2	Clay (Fe^{3+} h.s.)	59.34	0.327(5)	0.579(9)	0.403(14)	
			Silicate (Fe^{2+} h.s.)	40.66	1.111(14)	2.553(27)	0.598(40)	
	18–21	1992.7	Clay (Fe^{3+} h.s.)	55.62	0.287(269)	0.586(529)	0.613(68)	
			Silicate (Fe^{2+} h.s.)	44.38	1.182(349)	2.396(696)	0.629(73)	
	21–24	1990.2	Clay (Fe^{3+} h.s.)	73.12	0.308(18)	0.545(29)	0.404(47)	
			Silicate (Fe^{2+} h.s.)	26.88	1.219(21)	2.759(42)	0.253(61)	
	24–27	1987.7	Clay (Fe^{3+} h.s.)	53.23	0.307(6)	0.622(10)	0.473(13)	
			Silicate (Fe^{2+} h.s.)	43.00	1.101(14)	2.450(26)	0.727(37)	
			Hematite	3.76	0.346(55)	−0.200(10)	0.331(13)	50.02(30)
	27–30	1985.2	Clay (Fe^{3+} h.s.)	59.39	0.257(131)	0.494(226)	0.611(125)	
			Silicate (Fe^{2+} h.s.)	40.61	1.147(250)	2.261(491)	0.752(195)	

	30–33	1982.7	Clay (Fe^{3+} h.s.)	64.22	0.307(9)	0.595(17)	0.578(24)	
			Silicate (Fe^{2+} h.s.)	35.78	1.163(13)	2.312(74)	0.570(70)	
	33–36	1980.1	Clay (Fe^{3+} h.s.)	59.10	0.325(7)	0.605(13)	0.493(18)	
			Silicate (Fe^{2+} h.s.)	40.90	1.124(15)	2.490(30)	0.648(39)	
	36–39	1977.6	Clay (Fe^{3+} h.s.)	47.78	0.324(4)	0.587(8)	0.486(11)	
			Silicate (Fe^{2+} h.s.)	34.68	1.141(8)	2.491(16)	0.591(26)	
			Hematite	17.54	0.342(55)	−0.199(108)	1.094(205)	49.34(45)
Non-dredged trench (Point B)	0–3	–	Clay (Fe^{3+} h.s.)	39.33	0.337(3)	0.590(6)	0.441(8)	
			Silicate (Fe^{2+} h.s.)	36.40	1.131(5)	2.458(10)	0.573(18)	
			Hematite	24.27	0.372(32)	−0.219(62)	1.139(120)	48.92(25)
	3–6	–	Clay (Fe^{3+} h.s.)	39.53	0.325(5)	0.613(9)	0.397(11)	
			Silicate (Fe^{2+} h.s.)	43.97	1.144(9)	2.457(18)	0.635(28)	
			Hematite	16.50	0.373(45)	−0.191(90)	0.852(179)	50.36(36)
	6–9	–	Clay (Fe^{3+} h.s.)	44.97	0.320(2)	0.587(3)	0.349(4)	
			Silicate (Fe^{2+} h.s.)	37.12	1.112(3)	2.533(6)	0.468(13)	
			Hematite	17.92	0.395(40)	−0.308(79)	1.067(153)	48.84(31)

Fig. 3 Eh-pH diagram of iron optimized at sampling sites

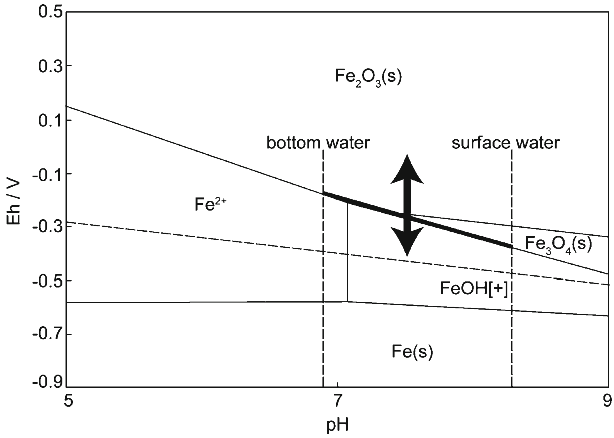

generation at point A is shown in Fig. 3. The conditions for hematite generation at points A and B, indicated by the arrows in the figure, occur when the environment exceeds an Fe_2O_3–FeOH[+] boundary. For Eh in the seawater to become suitable for hematite generation, that is, to exceed the Fe_2O_3–FeOH[+] boundary in the diagram, it is reasonable to assume that the amount of DO increases. Theoretically, if the amount of DO is low in all the seawater, the Eh in the seawater will not be less than at least −200 mV. Since hematite was generated at all depths at non-dredged point B, which is a short distance from point A (ca. 500 m), the possibility that the iron concentration in the supplied seawater was low around point A becomes very small.

The radiation dose of excess ^{210}Pb at point A indicated that the sedimentation rate is 1.2 cm·year^{-1} (core average, MAR), and there was obviously no disturbance over the core. As the sedimentation rate in the inner part of Tokyo Bay was within 0.60 to 1.56 cm·year^{-1}, this was a reasonable value.

The sedimentation age of the core bottom layer (36–39 cm) at point A can be calculated from the slope as being around 1976 to 1979. Since the sedimentation age of the bottom occurs after the dredging, the core at point A is accumulated after the dredging. The sedimentation age of the layers in which the hematite was measured corresponds to the years 1976–1979, 1986–1989 and 2006–2009. Therefore, at those times, the Eh was clearly sufficient to generate hematite. As shown in Fig. 1, the DO in 1976–1979 and 1986–1989 did not fall to 0 mg·L^{-1} in summer, suggesting that the high Eh in seawater persisted through each year. Although the DO data for 2006–2009 are inconclusive, it is possible that the surface hematite that was oxidized by the air was observed. However, in the layers representing at least two of the time periods, proof of weakened hypoxia was clearly recorded in the sediment. Therefore, the agreement between the quality of hematite in sediment and past DO representing hypoxia has been confirmed. Since this method is very simple, it serves as a good index by which the scale of past hypoxia can be evaluated in other dead zones.

Acknowledgement This work was supported by a Grant-in-Aid for Young Scientists Start-up (20810007).

References

1. Diaz, R.J., Rosenberg, R.: Science **321**, 926–929 (2008)
2. Bale, C.W., Chartrand, P., Degtrev, S.A., Eriksson, G., Hack, K., Ben Mahfoud, R., Melancon, J., Pelton, A.D., and Petersen, S.: FactSage thermochemical software and databases. Calphad **26**, 189–228 (2002)
3. Sasaki, J., Kawamoto, S., Yoshimoto Y., Ishii, M. Kakino, J.: J. Coastal Res. **56**, 890–894 (2009)
4. Kanai, Y.: Appl. Radiat. Isot. **69**, 455–462 (2011)